Wing-Wing Interference Effects for Cruciform Missiles

M. S. Miller*
Dynetics, Inc., Huntsville, Alabama
and
J. E. Burkhalter†
Auburn University, Alabama

Experimental results obtained from an investigation of aerodynamic characteristics of a cruciform missile in subsonic flow are presented. The data, obtained from wind-tunnel tests of an instrumented pressure model of a cruciform missile, are used to quantitatively determine fin-fin interference effects on a cruciform missile when it is arbitrarily rolled and pitched. Results show that fin-fin interference effects are present at all roll angles, and are generally most significant on the inboard sections of each fin. Additionally, the suitability of an analytical technique based on planar lifting-surface theory to accurately model the flowfield is determined by comparison with experimental fin-pressure distributions and with sectional normal-force coefficients.

Nomenclature

b = wing span
B_{nm} = wing-loading coefficients
c = local wing chord
cc_n = sectional normal force/q_∞
C_p = pressure coefficient, $(p-p_\infty)/q_\infty$
C_R = root chord
C_T = tip chord
q_∞ = freestream dynamic pressure
S = wing planform area
u = freestream velocity component parallel to x axis
v = freestream velocity component parallel to y axis
w = nondimensional perturbation velocity parallel to z axis; freestream velocity component parallel to z axis
X/C = distance measured from the local leading edge of a fin divided by the local chord length

Subscripts

B = denotes angles measured relative to the body-axis coordinate system
nm = points or constants associated with the wing
LE = leading edge
w = angles measured relative to the wind-axis coordinate system
0 = wing-coordinate variables

Introduction

MOST missiles currently in existence are of the cruciform type and usually have lifting surfaces which are small, low-aspect-ratio fins of equal size and shape. In addition to providing lift, the four fins provide flight stability in both the horizontal and vertical directions. In most instances, cruciform missiles fly in either a "plus" orientation or a "cross" orientation. One of the characteristic features of a cruciform missile flying in the "plus" orientation is its ability to perform a maneuver in any plane without banking by deflecting only one set of control surfaces. However, for a missile flying in the "cross" orientation, both sets of control surfaces must be deflected to perform the same maneuver. Thus, a cruciform missile usually slides through a turn and does not roll as a turn is negotiated. This type of flight control, however, is neither the most efficient nor the most effective. For example, consider the pitch control of a cruciform missile with hinged fins at a zero roll angle. If both horizontal fins are deflected downward, an amount δ, then the result is an upward force F in the vertical plane. Now, if the same missile is rolled 45 deg and all four fins are deflected downward the same δ, a force equivalent to $\sqrt{2}\,F$ will be produced in the vertical plane. The result of rolling the missile is that the pitch effectiveness in the vertical plane has been increased significantly. Therefore, as Nielsen[1] points out, to obtain the largest force in response to a command for acceleration in a given plane, a cruciform missile must roll to a bank angle of 45 deg with respect to the given plane and then deflect all four fins. Since a missile has a low-mass moment of inertia in roll as compared to that in pitch, such a maneuver can increase the pitch control of a cruciform missile dramatically. For this reason, in addition to other factors, roll capability for a missile is a desirable feature.

It is easy to roll a cruciform missile with differential control surfaces, but prediction of the loading on each of the fins at a given roll angle and angle of attack is a difficult task. Chin[2] points out that because of the complex nature of the flow around a rolled missile, determination of the rolling moment is often omitted in preliminary design analyses since it is most conveniently evaluated in wind-tunnel tests.

When rolled (at a roll angle other than 45 deg), a missile loses its horizontal and vertical load symmetry and thus each of the four fins has different aerodynamic load distributions. The asymmetry resulting from the roll maneuver consequently causes an induced rolling moment which can have a significant effect on the missile guidance equipment. If the missile is allowed to roll freely, the guidance equipment may not operate properly if the roll rate exceeds certain limits. On the other hand, the guidance equipment may require the missile to be stabilized in roll, which in turn places demands on the control power available.

Apart from the interactions with the guidance system, both guided and unguided missiles can suffer from coupling

Presented as Paper 86-1772 at the AIAA 4th Applied Aerodynamics Conference, San Diego, CA, June 9–11, 1986; received Sept. 16, 1986; revision received Nov. 10, 1986.

*Associate Member of the Technical Staff. Member AIAA.
†Associate Professor, Aerospace Engineering. Member AIAA.

between roll rate and pitch rate which can lead to catastrophic instabilities. For example, if the aerodynamic center moves forward as the roll angle changes from 0 to 45 deg, and the missile rolls freely, a pitch oscillation linked to the roll rate can develop and lead to instability.[3] Both roll and pitch rates are controlled directly by individual fin loads and therefore it is desirable both to understand the flowfield around each fin on a cruciform missile and to be able to accurately predict these loads on each lifting surface when the missile is oriented at some arbitrary roll angle and angle of attack.

In both subsonic and supersonic flow, the unsymmetric fin loading when $\phi \neq 0.0$ or 45.0 deg is easy to visualize, but there are additional nonsymmetric loading factors due to fin-fin interference which are not as easily identified. It was therefore the purpose of the present research to obtain quantitative wing-wing interference wind-tunnel pressure data on a cruciform missile and compare the data with predictions from an analytical technique developed in Ref. 4.

This problem (analytically) lends itself to a vortex lattice solution which could be formulated to predict the unsymmetric fin loading. However, one would need to model all four fins, the body, and the roll orientation of the missile, which would require a very large matrix formulation. The lifting surface solution, on the other hand, is relatively easy to use and is readily adaptable to the cruciform missile with the exception of the fin-fin interference perturbations. Therefore, the lifting-surface algorithm was used for comparison purposes.

Theoretical Analysis

Basic Equations of Lifting-Surface Theory

In order to provide continuity, the basic equations of lifting-surface theory developed in Refs. 5 and 6 are presented as follows. For compressible flow, the downwash at an arbitrary point (x,y) on a planar wing due to an elemental area $dx_0 dy_0$ of a lifting surface can be expressed as

$$w(x,y) = \frac{1}{8\pi} \int_s \int \left\{ \frac{\Delta C_p(\xi,\eta)}{(y-y_0)^2} \times \left[+1 \frac{x-x_0}{\sqrt{(x-x_0)^2+\beta^2(y-y_0)^2}} \right] \right\} dx_0 dy_0 \tag{1}$$

where ξ and η are nondimensionalized chordwise and spanwise variables, respectively, defined as

$$\xi = \frac{x - x_{LE}(y)}{c(y)}, \qquad \eta = \frac{y}{b/2} \tag{2}$$

The assumed expression for the pressure loading can be written as

$$\Delta C_p(\xi,\eta) = \sum_{n=0}^{N} \frac{1}{c(\eta)} \sum_{m=0}^{M} [B_{nm} \sin(2m+1)\theta (\sqrt{(1-\xi)/\xi}\ \xi^n] \tag{3}$$

where

$$\theta = \cos^{-1}(\eta) \tag{4}$$

The B_{nm}'s are constant loading coefficients, $c(\eta)$ is the local chord, and M and N represent an arbitrary number of chordwise and spanwise control points, respectively. It can be easily shown that the above expression for ΔC_p produces a singularity at the leading edge of a wing, satisfies the Kutta condition at the trailing edge, and has slender wing behavior near a wing tip.

Now, if an element of the planform surface is sufficiently small, ΔC_p can be considered to be essentially constant and so can be taken outside the integral of Eq. (1). The resulting integral equation can be evaluated in closed form at the centroid of an element to give

$$\Delta w(x,y) = \frac{\Delta C_p(\bar{\xi},\bar{\eta})}{8\pi} [K(x_2,y_2) - K(x_2,y_1) - K(x_1,y_2) + K(x_1,y_1)] \tag{5}$$

where, for example,

$$K(x_1,y_1) = -\frac{(x-x_1)+\sqrt{(x-x_1)^2+\beta^2(y-y_1)^2}}{(y-y_1)} + \beta \ln [\beta(y-y_1)+\sqrt{(x-x_1)^2+\beta^2(y-y_1)^2}] \tag{6}$$

The other K's of Eq. (5) are evaluated by making the appropriate substitution of the subscripted variables in Eq. (6). A sketch of a wing and a subpanel element is shown in Fig. 1.

For small angles of attack, the boundary condition imposed is the requirement of no flow through the wing, i.e.,

$$w(x,y) + \sin\alpha(x,y) = 0 \tag{7}$$

Choosing spanwise and chordwise control point locations, the total downwash at any control point due to the entire wing is found by summing the effect of each subpanel of the wing surface. Thus, Eq. (7) becomes

$$\sum_s \sum \Delta w(x_i,y_j) + \sin\alpha(x_i,y_j) = 0 \tag{8}$$

where (x_i,y_j) are the control points positioned at desired locations. Equation (8), together with the defining relations (3) and (5), constitute a set of simultaneous linear algebraic equations for $(N) \times (M)$ unknown loading coefficients B_{nm}'s. Solving the set of equations for these coefficients allows one to compute the pressure loading at any point on the wing from Eq. (3).

Body Modeling

Body interference effects are known to play an important role in the loading of missile fins. The presence of a body causes an upwash on the fin which creates a slightly higher angle of attack at different spanwise locations. In order to model the flow as realistically as possible, body effects on the fins are accounted for by assuming that the body is cylindrically shaped. The cylinder is generated with a line of doublets whose axis is in the z direction perpendicular to the horizontal plane. The results of adding the body to the analysis simply adds another term to the sin α term in Eq. (8). Wing-body carryover loads are accounted for by extending the wing into the body to form an image wing. Both of these modeling schemes are well known, and their theoretical development may be found in Ref. 7.

Cruciform Configurations

Shown in Fig. 2 is the basic body axis coordinate system for a missile as used in the present analysis. The x axis is positive rearward and lies along the longitudinal missile axis. The y axis lies in the horizontal plane of symmetry, and the z axis lies in the vertical plane of symmetry when one exists.

For flow around a cruciform missile at some positive angle of attack and positive roll angle, the freestream velocity V_∞ can be broken down into three velocity components, u, v, and w, as shown in Fig. 2. When this is done, the wind axis angle of attack α_w and the roll angle ϕ can be resolved into a body axis angle of attack α_B and a body axis sideslip angle

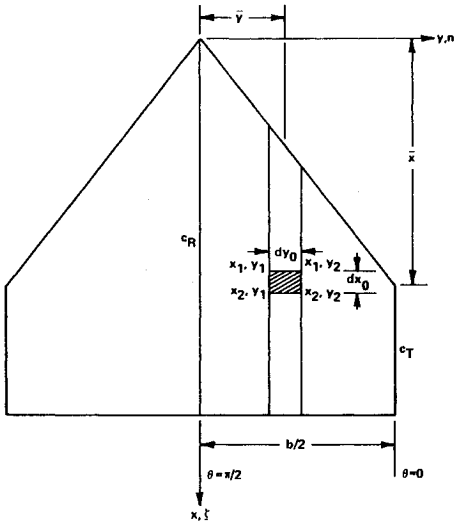

Fig. 1 Wing and subpanel coordinates.

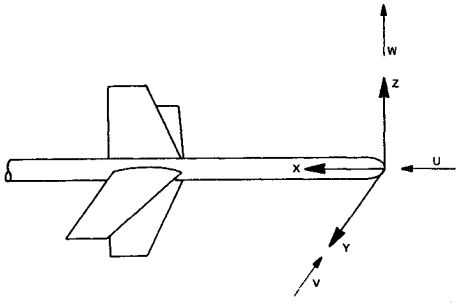

Fig. 2 Body axis coordinate system.

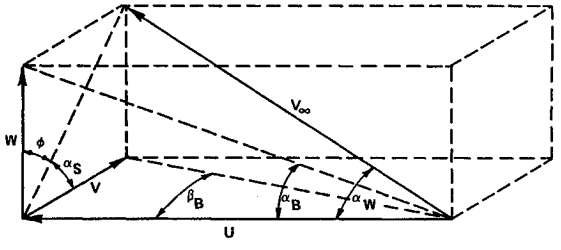

Fig. 3 Relationship between wind axis coordinate system and body axis coordinate system.

β_B.From Fig. 3, it can clearly be seen that

$$u = V_\infty \cos\alpha_w \tag{9}$$

$$v = -V_\infty \sin\alpha_w \sin\phi \tag{10}$$

$$w = V_\infty \sin\alpha_w \cos\phi \tag{11}$$

$$V_\infty{}^2 = u^2 + v^2 + w^2 \tag{12}$$

The body angle of attack and the body sideslip angle can therefore be written as

$$\alpha_B = \tan^{-1}(w/u) = \tan^{-1}[\tan\alpha_w \cos\phi] \tag{13}$$

and

$$\beta_B = \tan^{-1}(v/u) = -\tan^{-1}[\tan\alpha_w \sin\phi] \tag{14}$$

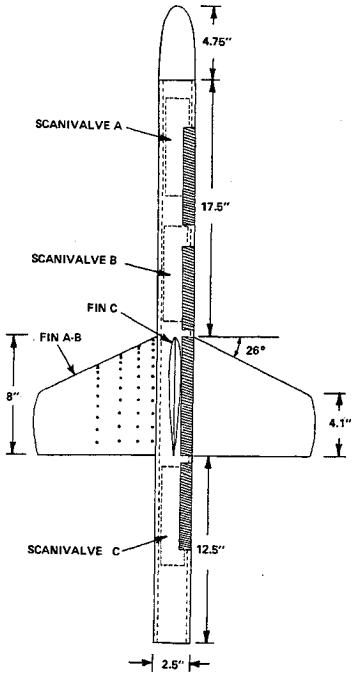

Fig. 4 Detailed sketch of experimental model.

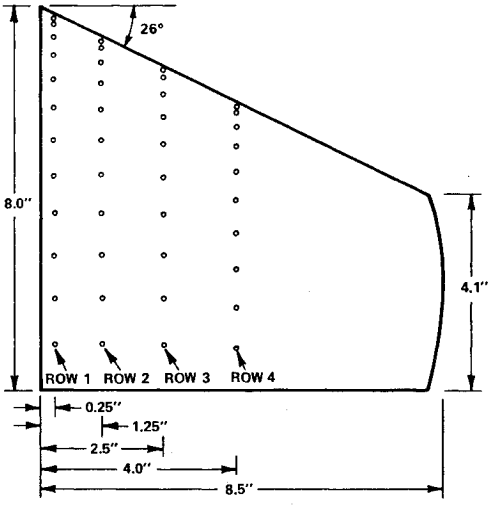

Fig. 5 Distribution of pressure ports across a fin surface.

Fin Loading

In this theoretical analysis, it is assumed that linear aerodynamics may be used and that fin loadings may be determined from component velocity vectors. From Figs. 2 and 3, the horizontal fin panels "see" an angle of attack α_B and the vertical fins "see" an angle of attack β_B. Thus, with these two angles known, the loading of both sets of fins due to "angle of attack" can be predicted using lifting-surface theory.

Careful inspection of Figs. 2 and 3 shows that there is an additional loading factor due to the velocity component v. The horizontal fins are sliding in the y direction at a velocity v and at a sideways angle of attack α_s. Using Fig. 3, this sideways angle of attack can be written as

$$\alpha_s = \tan^{-1}(w/v) = \tan^{-1}(-\cot\phi) \tag{15}$$

The same type of loading exists for the vertical fins due to the upwash velocity component w.

Prediction of the loading on the fins due to crossflow, or side flow, using lifting-surface theory is not as straightfor-

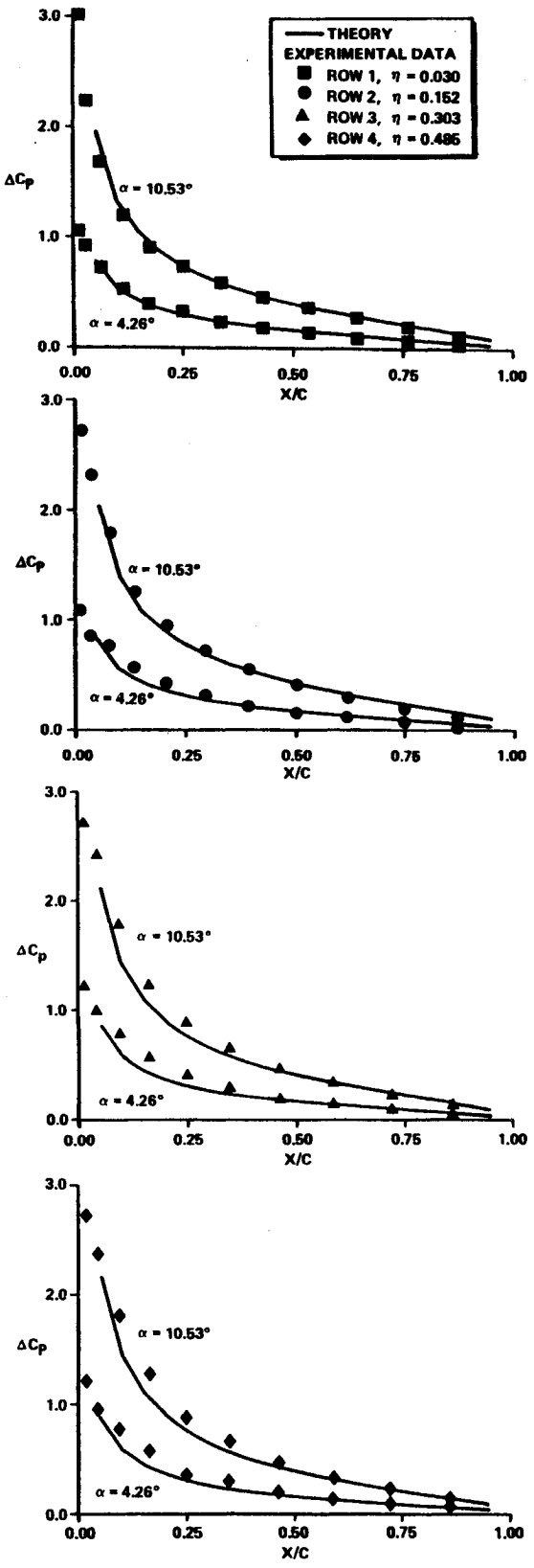

Fig. 6 Chordwise pressure variations on a horizontal fin, $\alpha =$ 4.26 deg and 10.53 deg.

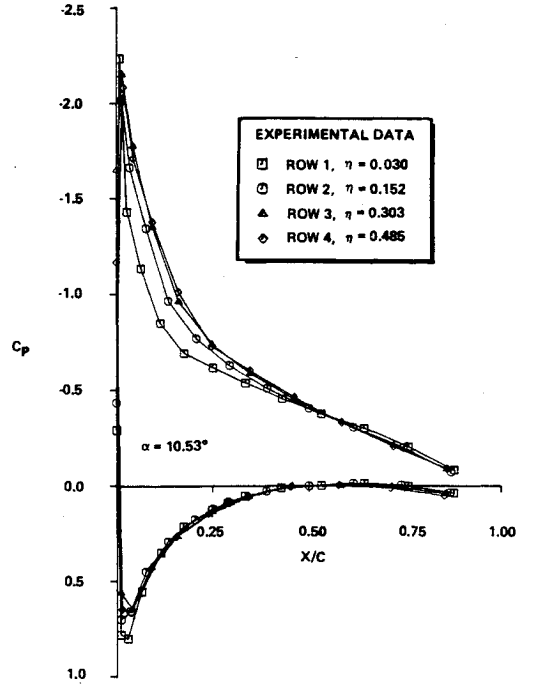

Fig. 7 Chordwise pressure distribution on a horizontal fin, $\alpha = 10.53$ deg.

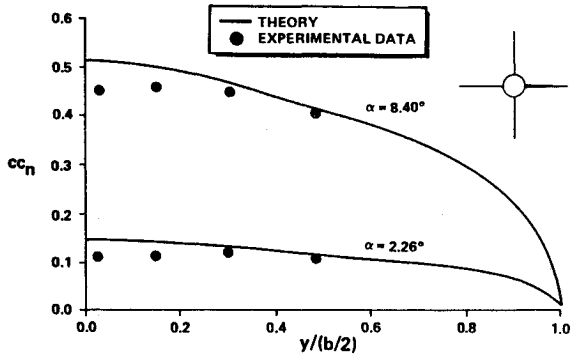

Fig. 8 Spanwise loading on a horizontal fin, $\alpha = 2.26$ deg and 8.40 deg.

ward as predicting the loads due to axial flow. When viewed from the side, the fin set is not symmetric. Therefore, the sideslip loading must be computed for a "left" wing panel which is radically different from the "right" panel. Because of this problem, the sideways analysis requires a manipulation of the wing geometry before the pressure solution can be obtained and added to the axial flow solution. This manipulation channels the locations at which pressures are computed in the body-fixed coordinate system through appropriate coordinate transformation and renondimensionalization equations, so that in the crossflow solution pressures are computed at the correct locations. This, however, is primarily a bookkeeping problem for the computer and does not alter the basic lifting-surface theory equations.[4]

Experimental Apparatus and Procedure

Experimental Model

In order to gain better insight into the flow around a cruciform missile at subsonic speeds as well as to provide verification of different analytical techniques, an experimental model of a cruciform missile was designed, fabricated, and subsonically tested. The model was 42.75 in. long and 2.5 in. in diameter. Three cutouts were made along the top portion of the fuselage to provide access for the installation and removal of three internal 48-port scanivalves. A single, noninstrumented fin was mounted on a fourth cutout so that the three additional fins could be bolted to the missile body from inside the fuselage. Shown in Fig. 4 is a dimensioned sketch of the model with the cutouts shaded in.

The fins of the missile, made of fiberglass, were formed to meet the geometrical requirements of a NACA-0010 airfoil.[8] Three separate fin surfaces were instrumented with a total of 137 pressure ports. One fin was instrumented on both sides

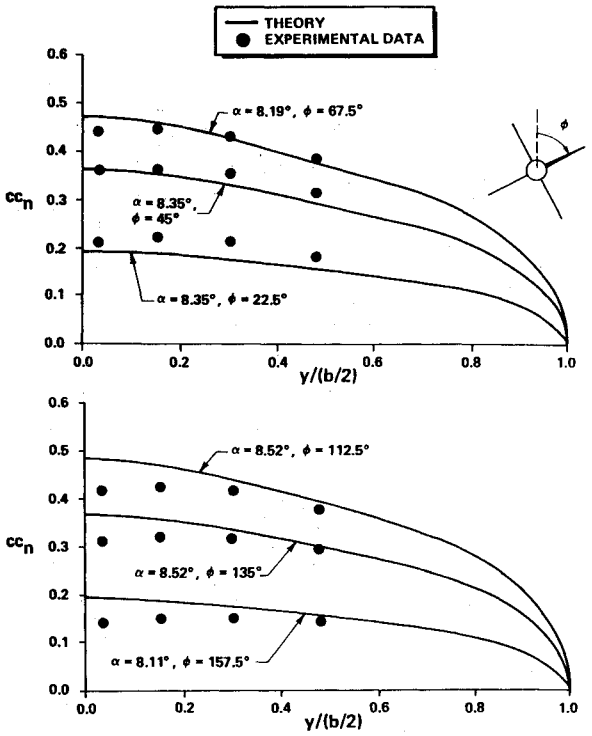

Fig. 9 Spanwise loading on a fin at various roll angles.

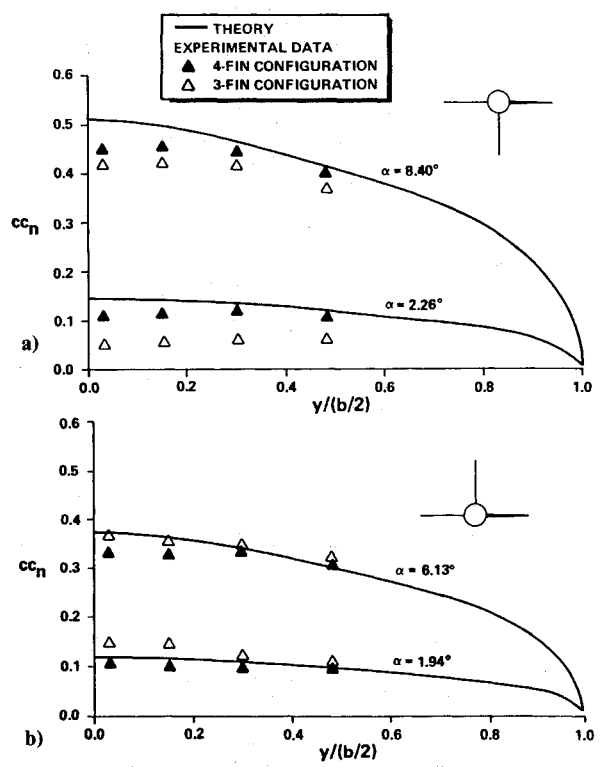

Fig. 10 Effects of a vertical fin on the spanwise loading of a horizontal fin. a) Top vertical fin, b) bottom vertical fin.

(fin A-B), while another fin adjacent to it was instrumented on only one side (fin C). The ports were distributed across each of the fin surfaces in four rows as shown in Fig. 5 using the cosine distribution

$$\frac{x}{c} = 1 - \cos\left[\frac{(n-1)\pi}{2N_p}\right] \tag{16}$$

where n is the port number, N_p the total number of ports in a row, x the distance from the local leading edge, and c the

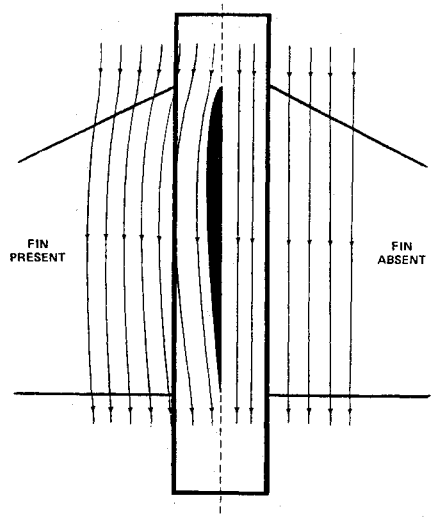

Fig. 11 Effect of a vertical fin on a flowfield.

local chord length. This cosine distribution placed the majority of the ports near the leading edge of the wing where the aerodynamic load changes are maximum. It should be noted that the same port distribution was used on all three instrumented surfaces.

Pressure lines were run from the pressure ports on the fin surfaces past the roots of each of the three fins to the pressure orifices on the scanivalves. An additional pressure line was connected to each scanivalve and run out the rear of the missile to provide calibration of the scanivalves without removing any of the cutouts. The model was designed so that each scanivalve was responsible for measuring all of the pressures on a particular fin surface. Additional details of the experimental model are contained in Ref. 9.

Test Results

Wind-tunnel tests of the missile in a four-fin configuration as well as a three-fin configuration were conducted at a Reynolds number of 160,000 (based on the body diameter of 2.5 in.). Data were obtained at each roll angle for an angle range from -6 to $+12$ deg in 2-deg increments. The geometrical angles of attack measured were corrected to account for tunnel wall constraints using the procedure detailed in Ref. 10.

It is appropriate to first compare the results of the analytical technique utilized in this research to the relatively simple case of a cruciform missile with a zero roll angle at a given angle of attack. At a zero roll angle, the aerodynamic loading on a missile is symmetric; thus, there are no pressure differences across the vertical fins, nor are there any crossflows present.

In Fig. 6, theoretical predictions of the chordwise pressure variations over a horizontal fin at two different angles of attack are compared with experimental data obtained from the four rows of pressure ports located on fin A-B. Overall, the agreement between the two is quite good. Data obtained from row one compare almost identically with theoretical predictions. As the spanwise distance away from the fuselage increases, the agreement between theoretical and experimental results for rows three and four tends to degrade, as might be expected.

Shown in Fig. 7 is the experimental pressure distribution obtained from the four rows of pressure ports located on fin A-B when the missile was at an angle of attack of 10.53 deg. From this figure, the magnitudes of the pressure coefficients along the top surface of the fin are seen to be significantly lower near the missile fuselage. Figure 8 presents experimental and theoretical sectional normal-force coefficient results for the spanwise loading on a horizontal fin at two different angles of attack. Once again, the reduction in loading near the missile fuselage can clearly be seen. The observed reduc-

tion in wing loading is believed to be due to the presence of fuselage interference on the flow over the fin. References 11 and 12 present similar results obtained from wind-tunnel tests of aircraft wing-body configurations which support this belief.

Several cases were run which included the effects of crossflow in the theoretical analysis. Comparisons were made for the case of maximum loading due to crossflow which occurred when fin A-B was rolled 45 deg downward from the horizontal position at a wind-axis angle of attack of 12.53 deg. There was some improvement in the accuracy of the theoretical prediction when crossflow was accounted for but the improvement was so small that it did not warrant its use. For this reason, crossflow effects were not included in comparisons of experimental and theoretical results. It is important to note, however, that when a missile is rolled and its control surfaces are deflected, crossflow effects may indeed be significant.

Comparisons of the spanwise loading on fin A-B obtained from wind-tunnel tests with theoretical predictions are shown in Fig. 9 for a range of roll angles. It is important to note in the figure the convention of roll-angle measurement as viewed from the rear of the missile. From Fig. 9 it is seen that for the most part, theoretical results are shown to slightly underpredict the actual spanwise loading on fin A-B when it is rolled 22.5, 45, and 67.5 deg from its vertical position. It can clearly be seen that as the roll angle increases from 22.5 to 67.5 deg, the difference between experimental and theoretical results reduces to very acceptable levels of agreement. Further inspection of Fig. 9 shows that good agreement between experimental and theoretical results continues to exist as fin A-B is rolled to an angle of 157.5 deg.

In an attempt to isolate wing-wing interference effects, the noninstrumented fin adjacent to fin A-B was removed. The model was then retested at various roll angles and angles of attack. Comparison of experimental results for both the three- and four-fin configurations shows that the presence of a fin can have a significant effect on the flow over a fin adjacent to it. Presented in Figs. 10, 12, and 14 are such comparisons along with theoretical predictions.

The results presented in Fig. 10 for the missile in the "plus" configuration can be summarized as follows. For positive angles of attack, the absence of the top vertical fin tends to decrease the spanwise loading on the horizontal fins while the absence of the lower vertical fin tends to increase the spanwise loading. For positive angles of attack it is postulated that the presence of the top vertical fin constricts the streamlines in the region above the horizontal fins as shown in Fig. 11. The constriction of the streamlines causes the velocity of the flow in that region to increase. The higher velocity in turn creates a lower pressure on the top surfaces of the horizontal fins. The increased loading seen in Fig. 10a with the top vertical fin present is a direct result of this lower pressure. The presence of the bottom vertical fin similarly constricts the streamlines in the region below the horizontal fins. The increase in velocity in turn creates a lower pressure. The result of this lower pressure acting on the bottom surfaces of the horizontal fins is to reduce the spanwise loading as shown in Fig. 10b.

If a missile fin is rotated downward from a horizontal position and the fin directly above it is removed, one might expect a *decrease* in loading on the rotated fin to occur similar to that experienced by a horizontal fin of a missile in a "plus" orientation. However, experimental results presented in Fig. 12 show that the result is a *higher* loading experienced by the fin rotated downward. The difference in loading between the three- and four-fin configurations is seen to significantly increase as the roll angle of the lower fin increases from 22.5 to 67.5 deg.

Careful inspection of the flow around the missile leads to the probable cause of this observed increase in loading. When a cruciform missile is in a "plus" orientation at some angle of attack, there is no pressure difference across the vertical fins. Thus, as verified from observations of the experimental model, no trailing vortices are shed off the tips of the vertical fins. However, when a cruciform missile is in a rolled position, all four fins are known to produce tip vortices.

Referring to Fig. 13, it is seen that if fin 1 is removed, a significant amount of the downwash experienced by fin 2 is eliminated. Thus, due to a reduction in downwash, fin 2 "sees" a higher angle of attack and, as a direct result of this higher angle of attack, the loading on fin 2 increases. The increase in the spanwise loading between the three- and four-fin configurations with the increase in roll angle can be explained as follows.

The loading on fin 1 is known to increase as the roll angle increases from 0 to 90 deg, and the strength of the tip vortex

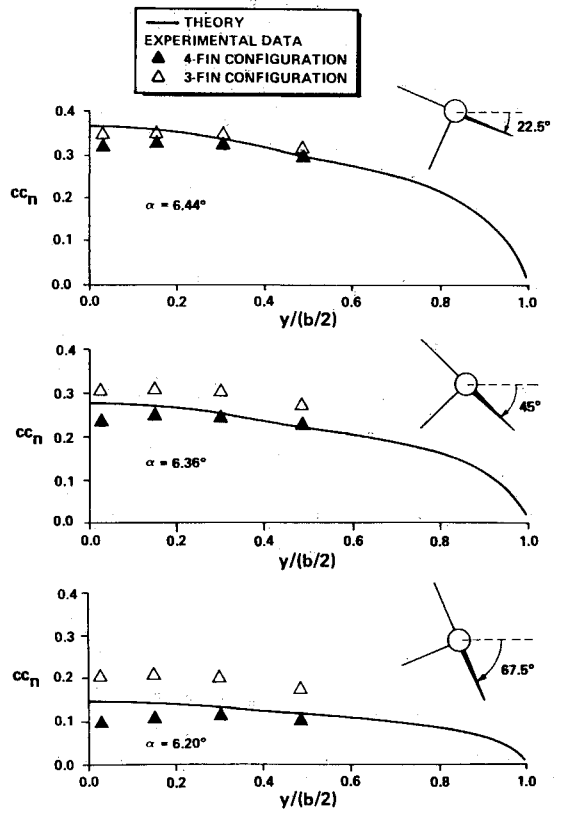

Fig. 12 Comparison of the spanwise loading for three- and four-fin configurations at various roll angles.

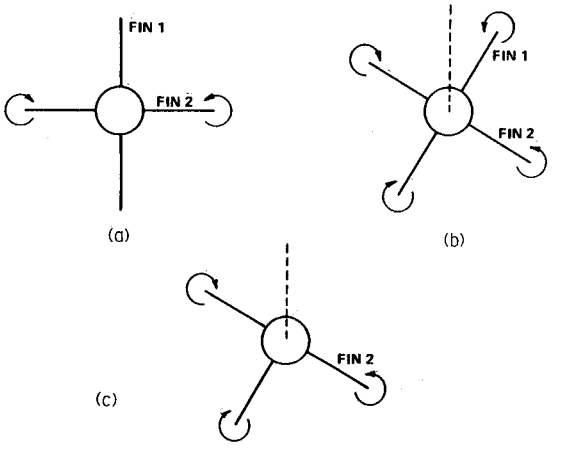

Fig. 13 Vortices produced by a cruciform missile. a) Plus orientation, b) rolled orientation, c) rolled orientation with fin removed.

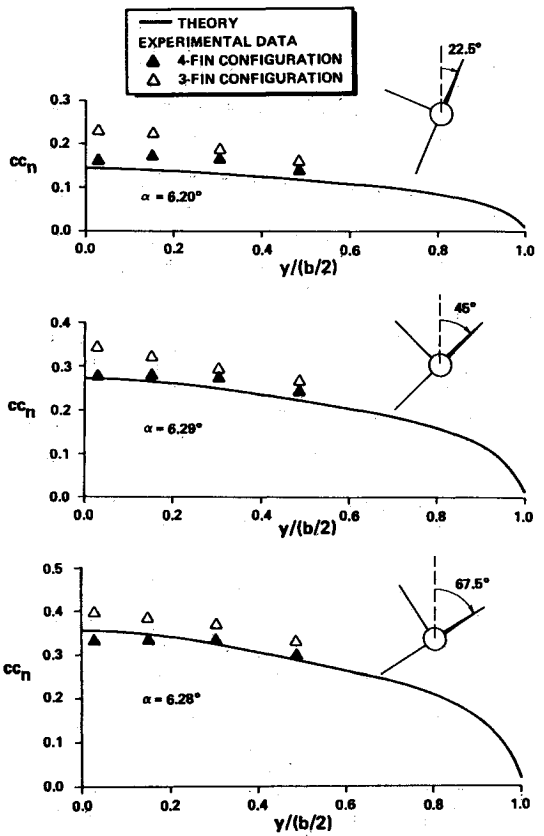

Fig. 14 Comparison of the spanwise loading for three- and four-fin configurations at various roll angles.

shed from fin 1 is directly proportional to the magnitude of the loading on the fin. Thus, the strength of the tip vortex is directly proportional to the roll angle. Hence, the removal of fin 1 at large roll angles eliminates more downwash than at smaller roll angles. The end result is that the difference in spanwise loading seen between the three- and four-fin configurations increases as the roll angle increases.

Presented in Fig. 14 are results obtained when the top vertical fin of the experimental model was rotated downward from a "plus" orientation with the fin directly below it removed. As before, the spanwise loading increases with removal of the lower fin. The difference in loading for the three outboard rows is observed to slightly increase as the fin is rotated downward. However, the difference in loading for the inboard row does not appear to be noticeably affected by the roll angle. The reasons for these observations are not clearly understood, but they can most likely be attributed to body-blanketing effects. In any case, removal of a fin, i.e., the elimination of fin-induced velocities, causes significant changes in adjacent fin loading, especially near the wing root.

Conclusions

The goal of this research was to obtain quantitative experimental wing-wing interference pressure data for a cruciform missile and to compare the data with predictions produced by a theoretical technique based on a planar lifting-surface theory. From the results presented, it has been shown that although the theoretical technique utilized does not account for fin-fin interference effects, good agreement between the experimental and theoretical results was obtained for a cruciform missile (with all four fins attached). Experimental results obtained from these tests have shown that the presence of a fin does have a significant effect on the loads produced by adjacent fins. The effect is large enough so that adjacent fin-induced loads cannot be ignored if accurate force and moment coefficients are to be computed. This is especially true for the rolling-moment computations.

References

[1]Nielsen, J. N., *Missile Aerodynamics,* McGraw-Hill, New York, 1960, p. 226.

[2]Chin, S. S., *Missile Configuration Design,* McGraw-Hill, New York, 1961, p. 122.

[3]Brebner, G. G., "The Control of Guided Weapons," AGARD-LS-98, Feb. 1979, pp. 7.1–7.29.

[4]Burkhalter, J. E., "Research on Detailed Prediction Techniques for Aerodynamic Coefficients," Interim Report on U.S. Army Contract DAAHO1-83-C-A150, Aerospace Engineering Department, Auburn University, Dec. 1984.

[5]Purvis, J. W. and Burkhalter, J. E., "Simplified Solution of the Compressible Lifting Surface Problem," *AIAA Journal,* Vol. 20, May 1982, pp. 589–597.

[6]Abernathy, J. M. and Burkhalter, J. E., "Load Distribution of Multielement Deformed Airfoils with Gap Effects," *Journal of Aircraft,* Vol. 19, Oct. 1982, pp. 831–838.

[7]Pitts, W. C., Nielsen, J. N., and Kaattari, G. E., "Lift and Center of Pressure of Wing-Body-Tail Combinations at Subsonic, Transonic, and Supersonic Speeds," NACA Rept. 1307, 1957.

[8]Abbott, I. H. and Von Doenhoff, A. E., *Theory of Wing Sections,* Dover Publications, New York, 1959, p. 315.

[9]Burkhalter, J. E. and Miller, M. S., "Surface Pressure Measurements on a Cruciform Missile in Subsonic Flow," Vol. 1, Auburn University Aerospace Engineering Technical Rept. 85-1, Sept. 1985.

[10]Pope, A., and Rae, W. H., *Low-Speed Wind Tunnel Testing,* Wiley, New York, 1984, pp. 344–444.

[11]Kuethe, A. M. and Chow, C. Y., *Foundations of Aerodynamics,* Wiley, New York, 1976, p. 172.

[12]Ashley, H. and Rodden, W. P., "Wing-Body Aerodynamic Interaction," *Annual Review of Fluid Mechanics,* Vol. 4, 1972, pp. 431–472.